

The Complex Dynamical Behavior of a Prey-Predator Model with Holling Type-III Functional Response and Non-Linear Predator Harvesting

Prahlad Majumdar, Surajit Debnath, Susmita Sarkar & Uttam Ghosh

To cite this article: Prahlad Majumdar, Surajit Debnath, Susmita Sarkar & Uttam Ghosh (2021): The Complex Dynamical Behavior of a Prey-Predator Model with Holling Type-III Functional Response and Non-Linear Predator Harvesting, International Journal of Modelling and Simulation, DOI: [10.1080/02286203.2021.1882148](https://doi.org/10.1080/02286203.2021.1882148)

To link to this article: <https://doi.org/10.1080/02286203.2021.1882148>



Published online: 10 Apr 2021.



Submit your article to this journal



Article views: 46



View related articles



View Crossmark data



Citing articles: 1 View citing articles



The Complex Dynamical Behavior of a Prey-Predator Model with Holling Type-III Functional Response and Non-Linear Predator Harvesting

Prahlad Majumdar, Surajit Debnath, Susmita Sarkar and Uttam Ghosh

Department of Applied Mathematics, University of Calcutta, Kolkata, India

ABSTRACT

In the present paper we have investigated the impact of predator harvesting in a two-dimensional prey-predator model with Holling type III functional response. The main objective of this paper is to study the change of dynamical behaviour of the prey-predator model in the presence of non-linear predator harvesting. The model system shows complex dynamics with the change of different system parameters. We have established the positivity and boundedness of the solutions under a certain parametric condition with non-negative initial conditions. The existence and stability criterion of different equilibrium points are investigated in terms of system parameters. We have shown that the system undergoes through saddle-node bifurcation, transcritical bifurcation, Hopf bifurcation and Bogdanov-Takens bifurcation under different parametric conditions. The structural changes or the system bifurcations predict the global dynamics of the model system. We have computed the first Lyapunov number to find the direction of the Hopf-bifurcating periodic solution of the system. Using numerical simulation we have studied here the effect of conversion efficiency, protection of the environment to the prey population and non-linear predator harvesting on the model dynamics. Finally the paper is ended with some conclusions.

ARTICLE HISTORY

Received 12 August 2020

Accepted 25 January 2021

KEYWORDS

Non-linear harvesting;
Holling type III functional
response; bogdanov-Takens
bifurcation

AMSSUBJECT

CLASSIFICATION

37N25; 49J15; 92D30

1 Introduction

The dynamics of the classical prey-predator model have been studied to understand the biological significance in the ecological system. In the last few years, the prey-predator interaction models get more attention among researchers for descriptive and management purposes. The continuously growing demand for food and resources gives rise to an increased exploitation of several biological resources [1–3]. Also, the protection of the ecosystem is a great challenge to the researchers in the recent years. From these point of views, the exploitation of natural biological resources and the harvesting to the population are commonly practised in fishery, forestry and in wildlife management [4–6]. To control the extinction of biological resources and minimize the exploitation of renewable resources optimal harvesting is an important tool.

The prey-predator model systems are mainly used to describe the intra- and inter-species interaction of population for living and food [7,8]. The simplest predator-prey interaction model is the Lotka-Volterra Model [9,10]. Rosenzweig and Macarther [11] improved the realistic Lotka-Volterra model by introducing the growth of density-dependent prey population and the prey consumption by a predator is non-linear type.

Depending upon the environment and the type of species, the functional responses become different. To interpret the consumption of prey by the predator mathematically Holling proposed three types of functional responses those are Holling types I, II, III. These functional responses are functions of prey populations only [12–14]. Holling type I functional response is fitted for the system where the prey population is available for a predator. But Holling type II and III both are monotonic increasing and show saturation effect when the number of prey is large. Holling type III functional response is mostly used when the number of predator encounters the prey population with a very lower amount due to unavailability of prey but when the prey becomes available then the response behaves like the Holling II type functional response. In most of the prey-predator model, it is assumed that the functional response is a monotonic increasing function of prey, because the presence of more prey in the environment is better for the predator [15,16]. Considering Holling type III functional response researchers have investigated different types of prey-predator model and fitted their results with real data [17–19]. Andrew Morozov [17] studied a prey-predator model of Holling type III functional response to investigate the dynamics of zoo-

plankton and predicted the emergence of Holling type III response to be facilitated in deep-water ecosystems. Dubey et al. [20] and Jiang et al. [18] have investigated prey-predator models with Holling type III functional response on phytoplankton, zoo-plankton and fish species. Alexander et al. [19] have studied a mathematical model of prey-predator overlap induced Holling type III functional response for the north sea cod *Gadus morhua* and whiting *Merlangius merlangus* populations.

In a prey-predator model, the harvesting of the prey or predator population is of great interest from the economical and biological point of view [21–23]. The harvesting of prey or predator population or both the population has a strong impact on the dynamics of the model system. Also, to control the predator population or to prevent the prey species from extinction due to predation, harvesting of the predator is used. The severity of the impact, depending on the used harvesting policy, may range from rapid depletion to complete preservation of a population. Many researchers have analysed a lot of prey-predator models using different types of harvesting by considering growth depending upon the species and their interaction [24–27]. Lin and Ho [28] proposed a modified Leslie-Gower prey-predator model with Holling type II functional response and time delay and analysed the local and global stability of the model. Li and Xiao [29] studied the bifurcation analysis for a Leslie-Gower prey-predator model with Holling type III functional response. Zhang et al. [30] analyzed the persistence and global stability for the Leslie-Gower predator-prey model with proportional harvesting to both the prey and predator population. Xiao and Ruan [22] analyzed the Bogdanov-Takens bifurcation for a prey-predator model with a constant rate of harvesting. Dai and Tang [31] studied the global stability of a prey-predator model with some functional response in the presence of a constant rate of prey harvesting.

Many researches have been carried out investigation of a prey-predator model with different types of functional responses and some other biological effects. It is clear from the literature review that there are only a very few research articles considering the prey-predator model with Holling type III functional response and predator harvesting together. To fill the gape, in this paper we are extending the work of Kar and Matsuda [32] replacing the linear predator harvesting by a non-linear one and eliminating the linear prey harvesting. In this paper we mainly focus on different bifurcations such as saddle-node, transcritical, Hopf and co-dimension two Bogdanov-Takens bifurcation. To study the complex dynamical behaviour we have

drawn two and three-dimensional bifurcation diagrams and extensively studied the nature of the system for values of the parameter in a different domain. The numerical results show that the predator harvesting rate, environmental protection to the prey and conversion efficiency plays an important role in model dynamics.

The rest of the part of this article is organized in the following way: the proposed model is formulated in section 2 and the positivity, boundedness of the solutions of the model system is presented in section 3. The existence of the feasible equilibrium points and their stability by parametric restriction are discussed in section 4. In section 5, we have analysed various types of bifurcations (transcritical, saddle-node, Hopf and Bogdanov-Takens's bifurcation) in the $h - \beta$ parametric plane. Finally, some numerical results and their discussion are given in section 6 and a brief conclusion is presented in section 7.

2 Model formulation

In 2007, Kar and Matsuda [32] proposed a deterministic mathematical model for the predator-prey interaction under the assumption that (i) the prey population grows logistically in the absence of a predator, (ii) the predator population dies out exponentially in the absence of prey population and (iii) the amount of prey consumed by a predator per unit time is a non-linear function of the prey density. Under the above assumption, the two-dimensional autonomous differential equation model for the prey-predator system is

$$\frac{dx}{dt} = rx\left(1 - \frac{x}{k}\right) - \frac{ax^2y}{b^2 + x^2} \quad (1a)$$

$$\frac{dy}{dt} = \frac{eax^2y}{b^2 + x^2} - my \quad (1b)$$

where $x(t)$ and $y(t)$ are the prey and predator density at time t ; r and k are the intrinsic growth rate and environmental carrying capacity of the prey population, m is the death rate of the predator population. Here, the term $\frac{ax^2y}{b^2 + x^2}$ represents the functional response of the predator to the prey, which is referred as the Holling type III functional response [33]. Here, a , b and e stands for the predator capture rate, half-saturation constant (some time call as the environmental protection coefficient to the prey population) and conversion factor denoting the number of newly born predators for each captured prey, respectively.

From an economical point of view, the harvesting function must be such that the harvesting agency gets

Table 1. The description of system variables and parameters with their dimension.

Symbol	Definition	Dimension
x	Prey density	biomass
y	Predator density	biomass
t	Time	time
r	Prey intrinsic growth rate	time ⁻¹
k	Prey carrying capacity	biomass
a	Maximum predation rate of predator	time ⁻¹
b	Environmental protection for the prey	dimensionless
e	Conversion efficiency of predator	dimensionless
m	Predator mortality rate	time ⁻¹
q	Catch-ability coefficient	dimensionless
E	Effort applied to harvest individuals	time ⁻¹
n_1	Suitable constant	time
n_2	Suitable constant	biomass ⁻¹

the maximum profit by using minimum efforts. Also, the agency desires that the harvesting should be continued for a long time without extinction of the economically important population. Naturally, the researchers use three types of harvesting which are stated below:

(i) the constant rate of harvesting $H_1(x) = H$, here a finite number of species are harvested per unit time [34,35].

(ii) proportional harvesting

$$H_2(x) = qEx$$

where q is the catch-ability co-efficient, E is the effort of harvesting for the species; which says that the number of species harvested per unit time is proportional to the number of species present at that time [23,36].

(iii) the non-linear harvesting (Holling type II harvesting)

$$H_3(x) = \frac{qEx}{n_1E + n_2x}$$

where q is the catch-ability co-efficient, E is the effort of harvesting for the species and n_1, n_2 are positive constants [37,38].

Kar and Matsuda [32] imposed linear proportional harvesting to both the prey and predator in the model system (1) and then the model reduces to the form

$$\frac{dx}{dt} = rx\left(1 - \frac{x}{k}\right) - \frac{ax^2y}{b^2 + x^2} - q_1E_1x \quad (2a)$$

$$\frac{dy}{dt} = \frac{eax^2y}{b^2 + x^2} - my - q_2E_2y \quad (2b)$$

They studied the local stability of the system. It has been observed that the linear proportional harvesting creates some unrealistic features such as the random search for the prey, unbounded linear growth of $H_2(x)$ with the increase of x or E or both [27]. The harvesting function $H_3(x)$ is more realistic because of its property. In this case $H_3(x)$ tends to $\frac{qE}{n_2}$ as x tends to infinity and $H_3(x)$

tends to $\frac{qx}{n_1}$ as E tends to infinity. Thus, the harvesting function $H_3(x)$ exhibits saturation effects with respect to both the stock abundance and the effort level. Also the parameter n_1 is proportional to the ratio of the stock level to the harvesting rate at a higher level of effort and n_2 is proportional to the ratio of the effort-level to the harvesting rate at higher stock levels.

In the model system (1) we assume that the predator population is economically important and we use the non-linear harvesting for the predator population. Thus, in presence of non-linear harvesting, the model system (1) becomes

$$\frac{dx}{dt} = rx\left(1 - \frac{x}{k}\right) - \frac{ax^2y}{b^2 + x^2} \quad (3a)$$

$$\frac{dy}{dt} = \frac{eax^2y}{b^2 + x^2} - my - \frac{qEy}{n_1E + n_2y} \quad (3b)$$

with the initial condition

$$x(0) \geq 0; y(0) \geq 0.$$

all the parameters are assumed to be positive from the biological point of view. The model parameters with dimension are described in Table 1.

Before going to the detailed analysis, to reduce the number of parameters we consider the following non-dimensional scheme for the above system of equation [39]:

$$\begin{aligned} x' &= \frac{x}{k}, y' = \frac{ay}{kr}, t' = rt, \beta = \frac{b}{k}, \delta = \frac{m}{r}, \alpha = \frac{ea}{r}, g \\ &= \frac{n_1Ea}{n_2kr}, h = \frac{aqE}{kr^2} \end{aligned}$$

Using the above non-dimensional scheme, we obtain the following system of differential equations

$$\frac{dx}{dt} = x(1 - x) - \frac{x^2y}{\beta^2 + x^2} \equiv xF_1(x, y) \quad (4a)$$

$$\frac{dy}{dt} = \frac{\alpha x^2y}{\beta^2 + x^2} - \delta y - \frac{hy}{g + y} \equiv yF_2(x, y) \quad (4b)$$

with the initial condition $x(0) \geq 0; y(0) \geq 0$.

Thus, from the biological point of view, we are interested in the dynamical behaviour of the model system (4) in the first quadrant of the $x - y$ plane, i.e.,

$$\mathbb{R}_+^2 = \{(x, y) \in \mathbb{R}^2 : x(0) \geq 0, y(0) \geq 0\}$$

In the next section we shall establish the positivity and boundedness of the solution of the proposed model. It is biologically important because of the feasibility and finiteness of the populations.

3 Positivity and boundedness of solutions

To discuss the positivity of the considered model system (4) we integrate the system equations in the range $(0, t)$, which gives

$$x(t) = x(0) \exp \left[\int_0^t \left[(1 - x(s)) - \frac{x(s)y(s)}{\beta^2 + x^2(s)} \right] ds \right]$$

$$y(t) = y(0) \exp \left[\int_0^t \left[-\delta + \frac{\alpha x(s)y(s)}{\beta^2 + x^2(s)} - \frac{hy(s)}{g + y(s)} \right] ds \right]$$

This shows that $x(t) \geq 0$ and $y(t) \geq 0$ whenever $x(0) \geq 0$ and $y(0) \geq 0$. Therefore, we can say that the solutions will remain in the first quadrant of the $x - y$ plane for the future infinite time starting from that first quadrant of the $x - y$ plane. Thus, any solution which starts in the first quadrant of the $x - y$ plane will remain in this plane. Hence, the state space of the system (4)

$$\mathbb{R}_+^2 = \{(x, y) \in \mathbb{R}^2 : x(0) \geq 0, y(0) \geq 0\}$$

is an invariant set.

Now, we shall prove that the solutions of the system (4) are bounded. For this purpose, let us assume that

$$w(t) = x(t) + \frac{1}{\alpha}y(t) \quad (5)$$

Then differentiating with respect to time, along the solution curve of the model system (4) we get

$$\begin{aligned} \frac{dw}{dt} &= \frac{dx}{dt} + \frac{1}{\alpha} \frac{dy}{dt} \\ &= x(1 - x) - \frac{x^2y}{\beta^2 + x^2} + \frac{x^2y}{\beta^2 + x^2} - \frac{\delta}{\alpha}y - \frac{hy}{\alpha(g + y)} \end{aligned} \quad (6)$$

Now, multiplying equation (5) by λ with $0 < \lambda < \delta$ and then adding with equation (6) we get

$$\frac{dw}{dt} + \lambda w = x(1 - x) - \frac{\delta}{\alpha}y - \frac{hy}{\alpha(g + y)} + \lambda x + \frac{\lambda}{\alpha}y.$$

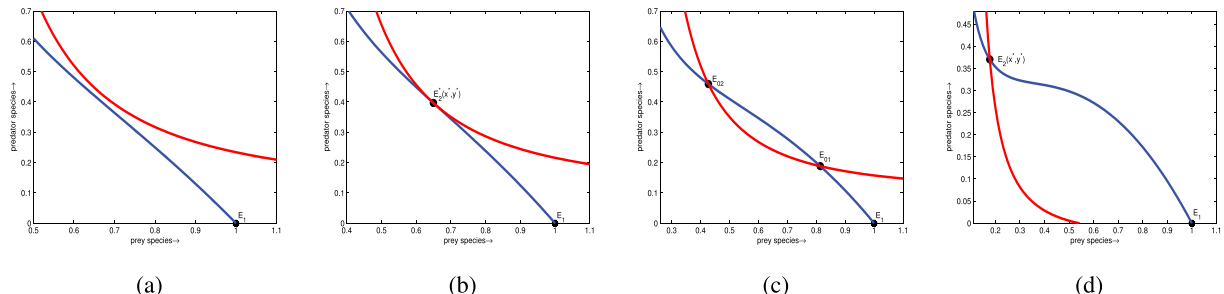


Figure 1. The position of different non-trivial equilibrium points of the model system (4) for different values of the parameters h and β as: (a) $h = 0.18$, $\beta = 0.6$ (b) $h = 0.18$, $\beta = 0.5598348639$, (c) $h = 0.18$, $\beta = 0.4$ and (d) $h = 0.1$, $\beta = 0.22$: when other parameter values are given in Table 2.

$$\leq x(1 - x + \lambda) + \frac{1}{\alpha}(\lambda - \delta)y.$$

Let $M = \max_{t \geq 0} \{x(1 - x + \lambda)\} = \frac{(\lambda+1)^2}{4}$ then we have

$$\frac{dw}{dt} + \lambda w \leq M$$

Then by using Gronwall's inequality we have,

$$x(t) + \frac{1}{\alpha}y(t) \leq \left(x(0) + \frac{1}{\alpha}y(0) \right) e^{-\lambda t} + \frac{M}{\lambda} (1 - e^{-\lambda t})$$

Since, $\lambda > 0$, so for any large value of t , we have

$$x(t) + \frac{1}{\alpha}y(t) \leq \frac{M}{\lambda} + \varepsilon$$

for any arbitrary positive ε .

Hence, from the positivity of $x(t)$ and $y(t)$, we can say that $x(t)$ and $y(t)$ are bounded and consequently the system (4) is dissipative.

4 Equilibria and stability analysis

In this section, we shall discuss the existence of various feasible equilibrium points of the system (4), which are the points of intersection of the prey zero growth isocline ($\frac{dx}{dt} = 0$) and predator zero growth isocline ($\frac{dy}{dt} = 0$) lying in the first quadrant of the $x - y$ plane (see Figure 1). The local stability of the equilibrium points and the global stability of the interior equilibrium points will be analyzed here.

4.1 Equilibria of the model system

The system (4) has three different types of equilibrium points, which are

- (i) the trivial equilibrium point $E_0(0, 0)$,
- (ii) the predator free or axial equilibrium point $E_1(1, 0)$, where the prey population is at its highest density level and

(iii) the co-existence interior equilibrium point $E_2(x^*, y^*)$ is the point of intersection of the lines $y = f_1(x) = (1-x)\frac{\beta^2+x^2}{x}$ and $y = f_2(x) = \frac{h(\beta^2+x^2)}{(\alpha-\delta)x^2-\delta\beta^2} - g$.

Solving the above equations, we get $y^* = \frac{(\beta^2\delta g + \delta g x^{*2} + \beta^2 h + h x^{*2} - \alpha g x^{*2})}{(\alpha x^{*2} - \beta^2 \delta - \delta x^{*2})}$ and x^* is the positive real solution of the following five-degree polynomial equation

$$\begin{aligned} x^5 - x^4 + A_2 x^3 + A_3 x^2 \\ + A_4 x + A_5 = 0 \end{aligned} \quad (7)$$

where,

$$A_2 = \frac{\alpha\beta^2 - 2\beta^2\delta - \alpha g + \delta g + h}{\alpha - \delta},$$

$$A_3 = \frac{-\alpha\beta^2 + 2\beta^2\delta}{\alpha - \delta},$$

$$A_4 = \frac{-\beta^4\delta + \delta^2\delta g + \beta^2 h}{\alpha - \delta},$$

$$A_5 = \frac{\beta^4\delta}{\alpha - \delta}$$

.

Since coefficients of equation (7) are functions of the model parameters, depending upon these parameters the system (4) may contain unique, two, coincident or no interior equilibrium points. If the coefficients A_2, A_3, A_4 and A_5 all are negative then the system (4) will contain an unique interior equilibrium point. If $h < h^{[SN]}$ (see Appendix-1(a) for the expression of $h^{[SN]}$) then the system (4) will contain two interior equilibrium points in the neighbourhood of this critical value, we name them as E_{01} and E_{02} (the density of predator population is higher at E_{02}). For $h = h^{[SN]}$ the two interior equilibrium points coincide, denote it by $E_2^*(x^*, y^*)$.

Table 2. The hypothetical value of the parameters for the model system (4).

α	β	δ	h	g
0.7	0.4	0.1	0.18	0.2

Table 3. The feasible equilibrium points in various sub-regions of Figure 2 and their nature.

Sub-region	Equilibrium Points	Nature of Equilibrium Points
R_1	E_0, E_1	saddle, stable node
R_2	E_0, E_1, E_{01}, E_{02}	saddle, stable node, saddle, stable spiral
R_3	E_0, E_1, E_{01}, E_{02}	saddle, stable node, saddle, unstable spiral (stable limit cycle)
R_4	E_0, E_1, E_{01}, E_{02}	saddle, stable node, saddle, unstable spiral (without limit cycle)
R_5	E_0, E_1, E_{01}	saddle, saddle, stable spiral
R_6	E_0, E_1, E_{01}	saddle, saddle, unstable spiral (stable limit cycle)

In the following **Table 2**, we have considered some hypothetical values of the parameter of the model system (4) to investigate all numerical results.

In **Figure 1**, we have shown the existence of various interior equilibrium points for the different values of the parameters h and β when other values of the parameters are fixed as given in **Table 2**. The **Figure 1(a)-(d)** represent respectively the existence of no interior equilibrium point, a unique coincident interior equilibrium point, pair of two distinct interior equilibrium points and only one interior equilibrium point.

4.2 Stability of the equilibrium point

Theorem 1. *The model system (4) has the trivial equilibrium point $E_0(0, 0)$ which is always unstable in nature.*

Proof. The variational matrix of the system (4) at the trivial equilibrium point $E_0(0, 0)$ is given by

$$J(E_0) = \begin{bmatrix} 1 & 0 \\ 0 & -\delta - \frac{h}{g} \end{bmatrix}$$

The eigenvalues of the variational matrix $J(E_0)$ are 1 and $-\delta - \frac{h}{g}$. Since, one eigenvalue of the variational matrix $J(E_0)$ is positive and other is negative. Then the trivial equilibrium point E_0 is always saddle i.e. unstable in nature. Hence for both the prey and predator population has no possibility of going to extinction. The characteristic of the equilibrium points in each of the sub-region are summarized in **Table 3**.

Theorem 2. *The model system (4) has the predator free axial equilibrium point $E_1(1, 0)$ where the prey population is at highest density level; is locally asymptotically stable if $h < h^{[TC]}$ and saddle point for $h > h^{[TC]}$ where $h^{[TC]}$ is defined in the proof.*

Proof. The variational matrix of the system (4) at the axial equilibrium point $E_1(1, 0)$ is given by

$$J(E_1) = \begin{bmatrix} -1 & -\frac{1}{1+\beta^2} \\ 0 & -\delta + \frac{\alpha}{1+\beta^2} - \frac{h}{g} \end{bmatrix}$$

The eigenvalues of the variational matrix $J(E_1)$ are -1 and $-\delta + \frac{\alpha}{1+\beta^2} - \frac{h}{g}$. Let $h^{[TC]} = g\left(-\delta + \frac{\alpha}{1+\beta^2}\right)$ with $\frac{\alpha}{1+\beta^2} > \delta$. If $h < h^{[TC]}$ then both the eigenvalues of the matrix $J(E_1)$ are negative, hence the axial equilibrium point E_1 is locally asymptotically stable and saddle for $h > h^{[TC]}$. \square

The variational matrix of the system (4) at the interior equilibrium point $E_2(x^*, y^*)$ is given by

$$J(E_2) = \begin{bmatrix} a_{11} & a_{12} \\ a_{21} & a_{22} \end{bmatrix}$$

where $a_{11} = 1 - 2x^* - \frac{2x^*y^*}{\beta^2+x^{*2}} + \frac{2x^{*3}y^*}{(\beta^2+x^{*2})^2}$, $a_{21} = \frac{2ax^*y^*}{\beta^2+x^{*2}} - \frac{2ax^{*3}y^*}{(\beta^2+x^{*2})^2}$, $a_{12} = -\frac{x^{*2}}{\beta^2+x^{*2}}$, and $a_{22} = -\delta + \frac{\alpha x^{*2}}{\beta^2+x^{*2}} - \frac{h}{g+y^*} + \frac{hy^*}{(g+y^*)^2}$.

Hence the characteristic equation of the variational matrix at the interior equilibrium point $E_2(x^*, y^*)$ is given by

$$\lambda^2 - C_1\lambda + C_2 = 0 \quad (8)$$

where $C_1 = \text{Trace}(J(E_2)) = a_{11} + a_{22}$ and $C_2 = \text{Det}(J(E_2)) = a_{11}a_{22} - a_{12}a_{21}$. If $C_1 < 0$, and $C_2 > 0$ then both the eigenvalues of $J(E_2)$ have negative real parts and hence the interior equilibrium point E_2 will be locally asymptotically stable.

In the next part of this section, we shall establish the conditions of global asymptotically stability of the interior equilibrium point $E_2(x^*, y^*)$ when it is locally asymptotically stable.

Theorem 3. *The interior equilibrium point $E_2(x^*, y^*)$ is globally asymptotically stable if $\frac{N^2x^*}{\beta^2} + (\delta + \frac{h}{g})y^* + (\frac{1+x^*}{2})^2 < x^* + \frac{\alpha v_1^2 y^*}{\beta^2+N^2}$, where $v_1 > 0$ is defined in the Appendix-I.*

Proof. To establish the global stability of the interior equilibrium point $E_2(x^*, y^*)$, we construct a Lyapunov function as follows,

$$L = \left(x - x^* - x^* \ln \frac{x}{x^*} \right) + \left(y - y^* - y^* \ln \frac{y}{y^*} \right)$$

Then differentiating the above equation with respect to t we get,

$$\frac{dL}{dt} = \left(\frac{x - x^*}{x} \right) \frac{dx}{dt} + \left(\frac{y - y^*}{y} \right) \frac{dy}{dt} \quad (9)$$

From the discussion of positivity and boundedness, we can assume that there exists a positive constant $N = \frac{M}{\lambda}$ satisfying $x(t), y(t) < N$, where $0 < \lambda < \delta$ and $M = \frac{(\lambda+1)^2}{4}$, and we assume that $v_1 > 0$ is the minimum value of $x(t)$.

Therefore after some algebraic computation equation (9) reduces to

$$\begin{aligned} \frac{dL}{dt} &= (x - x^*) \left[1 - x - \frac{xy}{\beta^2 + x^2} \right] \\ &\quad + (y - y^*) \left[\frac{\alpha x^2}{\beta^2 + x^2} - \delta - \frac{h}{g + y} \right] \\ &\leq (x - x^*)(1 - x) + \frac{\alpha x^* y}{\beta^2 + x^2} - \frac{\alpha x^2 y^*}{\beta^2 + x^2} - \delta y + \delta y^* \\ &\quad + \frac{h y^*}{g + y} \end{aligned}$$

$$\begin{aligned} &\leq - \left(x - \frac{1+x^*}{2} \right)^2 + \left(\frac{1+x^*}{2} \right)^2 - x^* + \frac{N^2 x^*}{\beta^2} \\ &\quad - \frac{\alpha v_1^2 y^*}{\beta^2 + N^2} + \delta y^* + \frac{h y^*}{g}. \end{aligned}$$

Now, $\frac{dL}{dt}$ will be less than zero if

$$\left(\frac{1+x^*}{2} \right)^2 - x^* + \frac{N^2 x^*}{\beta^2} - \frac{\alpha v_1^2 y^*}{\beta^2 + N^2} + \delta y^* + \frac{h y^*}{g} < 0$$

i.e.,

$$\frac{N^2 x^*}{\beta^2} + \left(\delta + \frac{h}{g} \right) y^* + \left(\frac{1+x^*}{2} \right)^2 < x^* + \frac{\alpha v_1^2 y^*}{\beta^2 + N^2}.$$

By using the Lasalle-Lyapunov invariance principle [40], the interior equilibrium point $E_2(x^*, y^*)$ is globally asymptotically stable

$$\text{if } \frac{N^2 x^*}{\beta^2} + \left(\delta + \frac{h}{g} \right) y^* + \left(\frac{1+x^*}{2} \right)^2 < x^* + \frac{\alpha v_1^2 y^*}{\beta^2 + N^2}.$$

Hence the proof is completed. \square

5 Bifurcation analysis

In this section we shall investigate different types of bifurcation analysis experienced by the model system (4). The qualitative behaviour of the solution changes depending on a parameter value in the neighbourhood of the bifurcation values. It has been shown that for changes in the values of certain parameter the vector field changes its structural behaviour and hence the system undergoes through different types of bifurcations. In the following subsections, we shall investigate the various types of bifurcations.

5.1 Transcritical bifurcation

In Theorem 2, we have observed that the axial equilibrium point E_1 is stable if $h < h^{[TC]}$ and is unstable if $h > h^{[TC]}$. Hence the system exchanges its stability at the critical value $h = h^{[TC]}$, i.e. a transcritical bifurcation occurs at the axial equilibrium point E_1 for the critical value of the parameter $h = h^{[TC]}$.

Theorem 4. The model system (4) undergoes through the transcritical bifurcation at $h = h^{[TC]}$ around the axial equilibrium point E_1 if the condition $h \neq \frac{4\alpha\beta^2\gamma^2}{2(1+\beta^2)^3}$ holds.

Proof. From the discussion in Theorem 2, we have observed that one of the eigenvalue of the Jacobian matrix $J(E_1)$ becomes zero when the system passes through the critical value $h = h^{[TC]}$. Then we are unable to justify the stability of the system by usual eigenvalue analysis method and we have to apply the Sotomayor's theorem [41] to overcome this problem.

Let, V and W be the eigenvectors corresponding to the zero eigenvalue of the matrix $J(E_1)$ and $[J(E_1)]^T$ respectively, then $V = \begin{pmatrix} v_1 \\ v_2 \end{pmatrix} = \begin{pmatrix} -\frac{1}{1+\beta^2} \\ 1 \end{pmatrix}$ and $W = \begin{pmatrix} w_1 \\ w_2 \end{pmatrix} = \begin{pmatrix} 0 \\ 1 \end{pmatrix}$.

Next, we consider $f(X, h) = [f_1(X, h), f_2(X, h)]^T$ where, $X = \begin{pmatrix} x \\ y \end{pmatrix}$ and $f_1(X, h) = x(1-x) - \frac{x^2y}{\beta^2+x^2}$, $f_2(X, h) = -\delta y + \frac{\alpha x^2 y}{\beta^2+x^2} - \frac{hy}{y+x}$.

Then we have $f_h(X, h = h^{[TC]})|_{E_1} = \begin{pmatrix} 0 \\ 0 \end{pmatrix}$, $Df_h(X, h = h^{[TC]})|_{E_1} = \begin{pmatrix} 0 & 0 \\ 0 & -\frac{1}{\gamma} \end{pmatrix}$

and

$$D^2f(X, h = h^{[TC]})(V, V)|_{E_1} = \begin{pmatrix} -\frac{2}{(1+\beta^2)^2} + \frac{4}{\beta^2(1+\beta^2)} \\ -\frac{4\alpha\beta^2}{(1+\beta^2)^3} + \frac{2h}{\gamma^2} \end{pmatrix}.$$

Therefore,

$$W^T f_h(X, h = h^{[TC]})|_{E_1} = 0,$$

$$W^T Df_h(X, h = h^{[TC]})|_{E_1} = -\frac{1}{\gamma} \neq 0,$$

$$\begin{aligned} W^T D^2f(X, h = h^{[TC]})(V, V)|_{E_1} \\ = -\frac{4\alpha\beta^2}{(1+\beta^2)^3} + \frac{2h}{\gamma^2} \neq 0 \text{ if } h \neq \frac{4\alpha\beta^2\gamma^2}{2(1+\beta^2)^3}. \end{aligned}$$

Hence, the transversality condition of the Sotomayor's theorem [41] for transcritical bifurcation is satisfied, i.e. the system (4) experiences transcritical bifurcation when h passes through the critical value $h = h^{[TC]}$.

Hence the theorem is proved. \square

It is clear from the above analysis that there is a critical value of the harvesting rate $h = h^{[TC]}$, the right side of which the predator population will go to extinction and only the prey population can exist. Thus from this analysis the theoretical biologist can give an estimate rate of harvesting per unit time to the

experimentalist/businessman such that the harvested species will not go to extinction.

5.2 Saddle-node bifurcation

Here we shall discuss the creation or destruction condition of two interior equilibrium points, i.e. the saddle node bifurcation analysis of the system for the interior equilibrium points. Since the coefficients of equation (7) can be considered as function of h , if we fix other model parameters then there exist a value of the parameter $h = h^{[SN]}$ (the expression of $h^{[SN]}$ is deduced in Appendix-II (a)) for which two roots of the equation (7) will coincide. In one side of the critical value the system has two interior equilibrium points and in other side has no interior equilibrium point. It can be easily shown that for this value of h , $\text{Det}(J(E_2^*)) = 0$ and consequently one root of the equation (8) will vanish (see Appendix-II (b)). Using Sotomayer's theorem [41,42], we shall establish that the system (4) experiences saddle-node bifurcation when the rate of harvesting h crosses the threshold value $h = h^{[SN]}$.

Theorem 5. The model system (4) goes through a saddle-node bifurcation at the coincident interior equilibrium point $E_2^*(x^*, y^*)$ when the rate of harvesting h crosses the critical value $h = h^{[SN]}$ if $(g_4a_{12}a_{22}^2 + g_6a_{12}a_{21}^2 + 2g_2a_{12}a_{22}^2) \neq (g_1a_{22}^3 + 2g_5a_{12}a_{21}a_{22})$ holds.

Proof. We have for the critical value $h = h^{[SN]}$ one root of the equation (8) vanishes i.e. one eigenvalue of the variational matrix $Df(X, h = h^{[SN]})$ at the interior equilibrium point $E_2^*(x^*, y^*)$ is zero and other is negative.

Let,

$$f(X, h) = [f_1(X, h), f_2(X, h)]^T$$

where $X = \begin{pmatrix} x \\ y \end{pmatrix}$, $f_1(X, h) = x(1-x) - \frac{x^2y}{\beta^2+x^2}$ and $f_2(X, h) = -\delta y + \frac{\alpha x^2 y}{\beta^2+x^2} - \frac{hy}{y+x}$.

Hence, $f_h(X, h)|_{E_2^*} = \begin{pmatrix} 0 & -\frac{y^*}{g+y^*} \end{pmatrix}^T$ and

$$Df(X, h)|_{E_2^*} = \begin{pmatrix} a_{11} & a_{12} \\ a_{21} & a_{22} \end{pmatrix}, \quad \text{where}$$

$$a_{11} = 1 - 2x^* - \frac{2x^*y^*}{\beta^2+x^{*2}} + \frac{2x^{*3}y^*}{(\beta^2+x^{*2})^2}, \quad a_{12} = -\frac{x^{*2}}{\beta^2+x^{*2}}, \quad a_{21} = \frac{2\alpha x^{*3}y^*}{\beta^2+x^{*2}} - \frac{2\alpha x^{*3}y^*}{(\beta^2+x^{*2})^2} \quad \text{and} \quad a_{22} = -\delta + \frac{\alpha x^{*2}}{\beta^2+x^{*2}} - \frac{h}{g+y^*} + \frac{hy^*}{(g+y^*)^2}.$$

The eigenvector corresponding to the eigenvalue zero of the matrix $Df(X, h = h^{[SN]})|_{E_2^*}$ is $V = \begin{pmatrix} v_1 \\ v_2 \end{pmatrix} = \begin{pmatrix} -a_{22} \\ a_{21} \end{pmatrix}$ and the eigenvector corresponding to the eigenvalue zero of the transpose of matrix

$$Df(X, hh^{[SN]})|_{E_2^*} \text{ is } W = \begin{pmatrix} w_1 \\ w_2 \end{pmatrix} = \begin{pmatrix} -a_{22} \\ a_{12} \end{pmatrix}.$$

Now we have,

$$D^2f(X, h)(V, V)|_{E_2^*} = \begin{pmatrix} g_1 a_{22}^2 - 2g_2 a_{21} a_{22} + g_3 a_{21}^2 \\ g_4 a_{22}^2 - 2g_5 a_{21} a_{22} + g_6 a_{21}^2 \end{pmatrix},$$

$$\text{where } g_1 = -2 - \frac{2y}{\beta^2 + x^{*2}} + \frac{10x^{*2}y}{(\beta^2 + x^{*2})^2} - \frac{8x^{*4}y}{(\beta^2 + x^{*2})^3},$$

$$g_2 = -\frac{2x^*}{\beta^2 + x^{*2}} + \frac{2x^{*3}}{(\beta^2 + x^{*2})^2}, g_3 = 0,$$

$$g_4 = \frac{2\alpha y^*}{\beta^2 + x^{*2}} - \frac{10\alpha x^{*2}y^*}{(\beta^2 + x^{*2})^2} + \frac{8\alpha x^{*4}y^*}{(\beta^2 + x^{*2})^3},$$

$$g_5 = \frac{2\alpha x^*}{\beta^2 + x^{*2}} - \frac{2\alpha x^{*3}}{(\beta^2 + x^{*2})^2}, g_6 = \frac{2h}{(g+y^*)^2} - \frac{2hy^*}{(g+y^*)^3}.$$

Then $W^T f_h(X, h = h^{[SN]})|_{E_2^*} = -a_{12} \frac{y^*}{g+y^*} \neq 0$ and also

$$W^T D^2 f(X, h = h^{[SN]})|_{E_2^*} = (g_4 a_{12} a_{22}^2 + g_6 a_{12} a_{21}^2 + 2g_2 a_{12} a_{22}^2) - (g_1 a_{22}^3 + 2g_5 a_{12} a_{21} a_{22}) \neq 0 \text{ if the conditions stated in the theorem are satisfied.}$$

Therefore, the system (4) goes through a saddle-node bifurcation around the interior equilibrium point $E_2^*(x^*, y^*)$ with respect to the bifurcation parameter h for the critical value of $h = h^{[SN]}$.

Hence the theorem is proved.

Biologically this bifurcation is of highly significant because if we cross the critical harvesting value $h = h^{[SN]}$, then co-existing interior equilibrium point arises i.e. on one side the predator population goes to extinction due to harvesting and in the other, both the species coexist.

5.3 Hopf bifurcation

Now, we shall study the Hopf bifurcation of the system around the interior equilibrium point $E_2(x^*, y^*)$ with respect to the system parameter h . Suppose at $h = h^*$ both the roots of the equation (8) are purely imaginary. This will happen if $C_1 = Tr(J(E_2)) = 0$ and $C_2 = Det(J(E_2)) > 0$. If in one side of $h = h^*$ the interior equilibrium point is stable spiral and in other side it is an unstable spiral then the system may experience the Hopf bifurcation.

Theorem 6. *The system (4) exhibits Hopf bifurcation about the interior equilibrium point $E_2(x^*, y^*)$ with respect to the parameter h at $h = h^*$ if $\frac{d}{dh} Tr(J(E_2))|_{h=h^*} \neq 0$.*

Proof. Since the variational matrix of the system (4) at the interior equilibrium point $E_2(x^*, y^*)$ have zero trace value and positive determinant for $h = h^*$, the eigenvalues of the variational matrix are purely imaginary. Hence, from the implicit function theorem [41] a Hopf

bifurcation occurs around $E_2(x^*, y^*)$ where a periodic orbit is created as the stability of the equilibrium point $E_2(x^*, y^*)$ changes. Hence, it is clear from the above analysis that under the parametric conditions (a) $Tr(J(E_2)) = 0$, (b) $Det(J(E_2)) > 0$ and (c) $\frac{d}{dh} Tr(J(E_2)) \neq 0$ at the critical value of the Hopf bifurcation parameter $h = h^*$.

Now, our aim is to investigate the stability direction of Hopf bifurcation of the system (4) describing above by computing the first Lyapunov coefficient. For this purpose, we shall translate the system (4) using the translation $x = \bar{x} + x^*$ and $y = \bar{y} + y^*$. Then the system (4) is transformed into

$$\begin{aligned} \bar{x} = & c_{10}\bar{x} + c_{01}\bar{y} + c_{20}\bar{x}^2 + c_{11}\bar{x}\bar{y} + c_{02}\bar{y}^2 + c_{30}\bar{x}^3 \\ & + c_{21}\bar{x}^2\bar{y} + c_{12}\bar{x}\bar{y}^2 + c_{03}\bar{y}^3 + \dots \end{aligned} \quad (10a)$$

$$\begin{aligned} \bar{y} = & d_{10}\bar{x} + d_{01}\bar{y} + d_{20}\bar{x}^2 + d_{11}\bar{x}\bar{y} + d_{02}\bar{y}^2 + d_{30}\bar{x}^3 \\ & + d_{21}\bar{x}^2\bar{y} + d_{12}\bar{x}\bar{y}^2 + d_{03}\bar{y}^3 + \dots \end{aligned} \quad (10b)$$

where the coefficient c_{ij} and d_{ij} are given in Appendix-III.

Since, the system goes through Hopf bifurcation, we get $c_{10} + d_{01} = 0$ and $\Delta = c_{10}d_{01} - c_{01}d_{10} \neq 0$. Now, we find the first Lyapunov number L^* , to determine the direction stability of limit cycle for the system (4), which is given by

$$\begin{aligned} L^* = & \frac{-3\pi}{2c_{01}\Delta^{\frac{1}{2}}} [c_{10}d_{10}(c_{11}^2 + c_{11}d_{02} + c_{02}d_{11}) \\ & + c_{10}c_{01}(d_{11}^2 + c_{20}d_{11} + c_{11}d_{02}) \\ & + d_{10}^2(c_{11}c_{02} + 2c_{02}d_{02})] \end{aligned}$$

$$\begin{aligned} & - 2c_{10}d_{10}(d_{02}^2 - c_{20}c_{02}) - 2c_{10}c_{01}(c_{20}^2 - d_{20}d_{02}) \\ & - c_{01}^2(2c_{20}d_{20} + d_{11}d_{20}) \end{aligned}$$

$$+ (c_{01}d_{10} - 2c_{10}^2)(d_{11}d_{02} - c_{11}c_{20}) - (c_{10}^2 + c_{01}d_{10})[3(d_{10}d_{03} - c_{01}c_{30})]$$

$$+ 2c_{10}(c_{21} + d_{12}) + (d_{10}c_{12} - c_{01}d_{21})]$$

If $L^* < 0$, the equilibrium point E_2 goes through supercritical Hopf bifurcation and for $L^* > 0$ the Hopf bifurcation is subcritical. \square

5.4 Bogdanov-Takens bifurcation

In the previous discussion of bifurcation analysis, we have investigated the occurrence of some co-dimension one bifurcation such as transcritical, saddle-node and Hopf bifurcation. In every case of these bifurcations, the bifurcation occurs for one significant bifurcation parameter. Now, our interest is to investigate the bifurcation of the model system (4) with respect to two parameters

which is known as the bifurcation of co-dimension two. The Bogdanov-Takens (BT) bifurcation is one of such kinds of bifurcation. For this purpose, we consider the two parameters β and h as the bifurcation parameters to establish the Bogdanov-Takens bifurcation. The point of Bogdanov-Takens bifurcation is a point where the saddle-node bifurcation curve and the Hopf bifurcation curve meet each other. The condition of Bogdanov-Takens bifurcation is $Tr[J(E_2)] = 0$ and $Det[J(E_2)] = 0$ at the interior equilibrium point $E_2(x^*, y^*)$ and for these conditions both of the eigenvalues of the variational matrix at $E_2(x^*, y^*)$ will be zero. Let us assume that for the critical value $\beta = \beta^{[BT]}$ and $h = h^{[BT]}$ the condition described above are satisfied. It is impossible to find the analytic expression of the values of $\beta = \beta^{[BT]}$ and $h = h^{[BT]}$ explicitly in the terms of other parameters and we will find them numerically. Now, we will deduce the normal form of the Bogdanov-Takens bifurcation for our proposed model system (4) with respect to the parameters β, h by using the procedure described in [43].

Theorem 7. *The model system (4) goes through the Bogdanov-Takens bifurcation in the small neighbourhood of $(\beta^{[BT]}, h^{[BT]})$ at the interior equilibrium point $E_2(x^*, y^*)$ when the conditions $Tr[J(E_2)]_{\beta=\beta^{[BT]}, h=h^{[BT]}} = 0$ and $Det[J(E_2)]_{\beta=\beta^{[BT]}, h=h^{[BT]}} = 0$ are satisfied.*

Also, if we perturbed the bifurcation parameters β, h of the model system (4) such that $\beta = \beta^{[BT]} + \eta_1$, $h = h^{[BT]} + \eta_2$ (where $|\eta_1|, |\eta_2| \ll 1$) in the neighbourhood of the Bogdanov-Takens bifurcation point then the system is topologically equivalent to the following model,

$$\varepsilon_1 = \varepsilon_2 \quad (11a)$$

$$\dot{\varepsilon}_2 = \zeta_1 + \zeta_2 \varepsilon_1 + \varepsilon_1^2 + s \varepsilon_1 \varepsilon_2 + O(\|\varepsilon\|^3) \quad (11b)$$

Moreover, the bifurcation curves are meeting to the Bogdanov-Takens bifurcation point in the $\eta_1 - \eta_2$ plane are represented as follows,

Saddle-node bifurcation curve: $SN = \{(\eta_1, \eta_2), 4\zeta_1(\eta_1, \eta_2) - (\beta_2(\eta_1, \eta_2))^2 = 0\}$
 Hopf bifurcation curve: $H = \{(\eta_1, \eta_2), \zeta_1(\eta_1, \eta_2) = 0, \zeta_2 < 0\}$,
 Homoclinic bifurcation curve: $HL = \{(\eta_1, \eta_2), \zeta_1(\eta_1, \eta_2) = -\frac{6}{25}(\zeta_2(\eta_1, \eta_2))^2, \zeta_2 < 0\}$.

Proof. To prove the above theorem, we have to deduce the normal form of the Bogdanov-Takens

bifurcation for the system (4) around the Bogdanov-Takens bifurcation point and also we shall obtain the analytic expression of saddle-node bifurcation curve, Hopf bifurcation curve and homoclinic bifurcation curve using the method defined in [43]. Using small perturbation of the parameters β, h as defined in the statement of the theorem the system (4) reduces to

$$\frac{dx}{dt} = x(1-x) - \frac{x^2y}{(\beta^{[BT]} + \eta_1)^2 + x^2} \quad (12a)$$

$$\frac{dy}{dt} = -\delta y + \frac{\alpha x^2 y}{(\beta^{[BT]} + \eta_1)^2 + x^2} - \frac{(h^{[BT]} + \eta_2)y}{y + y^*} \quad (12b)$$

Using the transformation $x = y_1 + x^*$, $y = y_2 + y^*$ to the system (12) we have,

$$\begin{aligned} \frac{dy_1}{dt} &= (y_1 + x^*)(1 - y_1 - x^*) \\ &\quad - \frac{(y_1 + x^*)^2(y_2 + y^*)}{(\beta^{[BT]} + \eta_1)^2 + (y_1 + x^*)^2} \\ &= f_1(y_1, y_2, \eta) \end{aligned} \quad (13a)$$

$$\begin{aligned} \frac{dy_2}{dt} &= -\delta(y_2 + y^*) + \frac{\alpha(y_1 + x^*)^2(y_2 + y^*)}{(\beta^{[BT]} + \eta_1)^2 + (y_1 + x^*)^2} \\ &\quad - \frac{(h^{[BT]} + \eta_2)(y_2 + y^*)}{(y + y_2 + y^*)} \\ &= f_2(y_1, y_2, \eta) \end{aligned} \quad (13b)$$

Expanding the system (13) in Taylor's series about the origin $(0, 0)$, we get the following expression:

$$\begin{aligned} \dot{y}_1 &= a(\eta)y_1 + b(\eta)y_2 + m_{00}(\eta) + m_{20}(\eta)y_1^2 \\ &\quad + m_{11}(\eta)y_1y_2 + m_{02}(\eta)y_2^2 + Q_1(y_1, y_2, \eta) \end{aligned} \quad (14a)$$

$$\begin{aligned} \dot{y}_2 &= c(\eta)y_1 + d(\eta)y_2 + n_{00}(\eta) + n_{20}(\eta)y_1^2 + n_{11}(\eta)y_1y_2 \\ &\quad + n_{02}(\eta)y_2^2 + Q_2(y_1, y_2, \eta) \end{aligned} \quad (14b)$$

where the coefficients $a(\eta), b(\eta), c(\eta), d(\eta)$ and m_{ij}, n_{ij} are given in Appendix-IV.

Let, at $\eta = 0$, the coefficient of the linear parts of (14) are respectively $a(0) = p_{11}, b(0) = p_{12}, c(0) = p_{21}$ and $d(0) = p_{22}$ and hence $J(E_2) = \begin{pmatrix} p_{11} & p_{12} \\ p_{21} & p_{22} \end{pmatrix}$ has eigenvalues 0, 0. Let $V_0 = \begin{pmatrix} p_{12} \\ -p_{11} \end{pmatrix}$, $V_1 = \begin{pmatrix} p_{12} \\ 1 - p_{11} \end{pmatrix}$; $W_1 = \begin{pmatrix} \frac{p_{11}}{p_{12}} \\ 1 \end{pmatrix}$, $W_0 = \begin{pmatrix} \frac{1-p_{11}}{p_{12}} \\ -1 \end{pmatrix}$ be the generalized eigenvectors corresponding to the repeated eigenvalues zero for the

matrix $J(E_2)$ and $[J(E_2)]^T$ respectively, where $J(E_2)V_0 = 0, J(E_2)V_1 = V_0, J(E_2)W_1 = 0$ and $J(E_2)W_0 = W_1$. Define the matrix $D = [V_0|V_1]$ which satisfies $D^{-1}J(E_2)D = \begin{pmatrix} 0 & 0 \\ 0 & 1 \end{pmatrix}$. Using the transformation $(y_1, y_2) = D(v_1, v_2) = (p_{12}(v_1 + v_2), -p_{11}v_1 + (1 - p_{11})v_2)$ the system (14) reduces to

$$\dot{v}_1 = (f(p_{12}(v_1 + v_2), -p_{11}v_1 + (1 - p_{11})v_2, \eta), W_0) \quad (15a)$$

$$\dot{v}_2 = (f(p_{12}(v_1 + v_2), -p_{11}v_1 + (1 - p_{11})v_2, \eta), W_1) \quad (15b)$$

Expanding the system (15) in Taylor's series about (v_1, v_2) we get the following:

$$\begin{aligned} \dot{v}_1 &= v_2 + k_{00}(\eta) + k_{10}(\eta)v_1 + k_{01}(\eta)v_2 + \frac{1}{2}k_{20}(\eta)v_1^2 \\ &\quad + k_{11}(\eta)v_1v_2 + \frac{1}{2}k_{02}(\eta)v_2^2 + Q_1(v_1, v_2, \eta) \end{aligned} \quad (16a)$$

$$\begin{aligned} \dot{v}_2 &= l_{00}(\eta) + l_{10}(\eta)v_1 + l_{01}(\eta)v_2 + \frac{1}{2}l_{20}(\eta)v_1^2 \\ &\quad + l_{11}(\eta)v_1v_2 + \frac{1}{2}l_{02}(\eta)v_2^2 + Q_2(v_1, v_2, \eta), \end{aligned} \quad (16b)$$

where $Q_1(v_1, v_2, \eta)$ and $Q_2(v_1, v_2, \eta)$ are the expression of the v_1, v_2 of order 3 or higher than 3. The constant k_{ij} and l_{ij} are given in Appendix-V. It is clear from the expressions of k_{ij} and l_{ij} that

$$k_{00}(0) = k_{10}(0) = k_{01}(0) = l_{00}(0) = l_{10}(0) = l_{01}(0) = 0$$

Now, we consider, $u_1 = v_1$ and

$$\begin{aligned} u_2 &= v_2 + k_{00}(\eta) + k_{10}(\eta)v_1 + k_{01}(\eta)v_2 + \frac{1}{2}k_{20}(\eta)v_1^2 \\ &\quad + k_{11}(\eta)v_1v_2 + \frac{1}{2}k_{02}(\eta)v_2^2 + Q_1(v_1, v_2, \eta) \end{aligned}$$

Then, equation (16) is transformed into

$$\dot{u}_1 = u_2 \quad (17a)$$

$$\begin{aligned} \dot{u}_2 &= g_{10}(\eta)u_1 + g_{01}(\eta)u_2 + g_{00}(\eta) + \frac{1}{2}g_{20}(\eta)u_1^2 \\ &\quad + g_{11}(\eta)u_1u_2 + \frac{1}{2}g_{02}(\eta)u_2^2 + \dots \end{aligned} \quad (17b)$$

Here, the g_{ij} 's are defined as follows:

$$\begin{aligned} g_{00}(0) &= g_{10}(0) = 0, & g_{20}(0) &= n_{20}(0), \\ g_{11}(0) &= m_{20}(0) + n_{11}(0), & g_{02}(0) &= n_{02}(0) + 2m_{11}(0), \end{aligned}$$

$$\begin{aligned} g_{00}(\eta) &= n_{00}(\eta) \dots, g_{10}(\eta) \\ &= c(\eta) + m_{11}(\eta)n_{00}(\eta) - n_{11}(\eta)m_{00}(\eta) + \dots \end{aligned}$$

$$\begin{aligned} g_{01}(\eta) &= d(\eta) + a(\eta) + m_{02}(\eta) - m_{11}(\eta) \\ &\quad + n_{02}(\eta)m_{00}(\eta) + \dots \end{aligned}$$

$$\begin{aligned} g_{11}(\eta) &= \frac{2n_{02}(\eta)a(\eta)}{b(\eta)} + 2m_{20}(\eta) + \frac{m_{11}(\eta)d(\eta)}{b(\eta)} \\ &\quad - \frac{m_{11}(\eta)a(\eta)}{b(\eta)} + \frac{2m_{02}(\eta)c(\eta)}{b(\eta)} - \frac{2m_{02}(\eta)d(\eta)}{b^2(\eta)} \\ &\quad - \frac{2m_{02}(\eta)a(\eta)d(\eta)}{b^2(\eta)} \end{aligned}$$

$$, \\ g_{02}(\eta) = 2\left(\frac{n_{02}(\eta)}{b(\eta)} + \frac{m_{11}(\eta)}{b(\eta)} + \frac{2m_{02}(\eta)a(\eta)d(\eta)}{b^2(\eta)}\right), \quad \text{where displayed terms are sufficient to compute the first partial derivatives of } g_{00}(\eta), g_{01}(\eta), g_{10}(\eta).$$

Now, we assume that, $k_{11}(0) = m_{20}(0) + m_{11}(0) \neq 0$ (BT ... 1) and make a parameter shift of coordinates in the u_1 -direction with $u_1 = w_1 + b(\eta)$, $u_2 = w_2$ where $b(\eta) \approx -\frac{k_{01}(\eta)}{k_{11}(\eta)}$ then the system (17) reduces to

$$\dot{w}_1 = w_2 \quad (18a)$$

$$\begin{aligned} \dot{w}_2 &= h_{00}(\eta) + h_{10}(\eta)w_1 + \frac{1}{2}h_{20}(\eta)w_1^2 + h_{11}(\eta)w_1w_2 \\ &\quad + \frac{1}{2}h_{02}(\eta)w_2^2 + \dots \end{aligned} \quad (18b)$$

where $h_{20}(0) = g_{20}(0), h_{11}(0) = g_{11}(0), h_{02}(0) = g_{02}(0)$ and the appropriate terms of h_{kl} are given by

$$\begin{cases} h_{00}(\eta) = g_{00}(\eta) + \dots \\ h_{10}(\eta) = g_{10}(\eta) - \frac{g_{20}(\eta)}{g_{11}(\eta)}g_{01}(\eta) + \dots \\ h_{02}(\eta) = g_{02}(\eta) + \dots \end{cases} \quad (19)$$

Now, we introduce a new variable τ by $dt = (1 + \phi w_1)d\tau$ and $\phi(\eta) = -\frac{h_{02}(\eta)}{2}$ then from (18) we have,

$$\dot{w}_1 = w_2 + \phi w_1 w_2 \quad (20a)$$

$$\begin{aligned} \dot{w}_2 &= h_{00} + (h_{10} + h_{00}\phi)w_1 + \frac{1}{2}(h_{20} + h_{10}\phi)w_1^2 \\ &\quad + h_{11}w_1w_2 + \frac{1}{2}h_{20}w_2^2 + \dots \end{aligned} \quad (20b)$$

Next, we use the transformation

$$\pi_1 = w_1$$

$$\pi_2 = w_2 + \phi w_1 w_2$$

The above transformation shift origin to the same point and using the transformation the system (20) reduces to

$$\dot{\pi}_1 = \pi_2 \quad (21a)$$

$$\dot{\pi}_2 = \kappa_1(\eta) + \kappa_2(\eta)\pi_1 + R(\eta)\pi_1^2 + S(\eta)\pi_1\pi_2 + \dots \quad (21b)$$

where $\kappa_1(\eta) = h_{00}(\eta)$, $\kappa_2(\eta) = h_{10}(\eta) - \frac{1}{2}h_{00}(\eta)h_{02}(\eta)$ and $R(\eta) = \frac{1}{2}(h_{02}(\eta) - h_{10}(\eta)h_{02}(\eta))$, $S(\eta) = h_{11}(\eta)$.

If the condition $R(0) = l_{20}(0) \neq 0$ (BT ... 2) satisfies then we can initiate a new time scaling (denote by t again) and new variables ε_1 and ε_2 are $t = |\frac{S(\eta)}{R(\eta)}| \eta$, $\varepsilon_1 = \frac{R(\eta)}{S^2(\eta)} \pi_1$ and $\varepsilon_2 = \text{sign}\left(\frac{S(\eta)}{R(\eta)}\right) \frac{R^2(\eta)}{S^3(\eta)} \pi_2$ in the coordinates $(\varepsilon_1, \varepsilon_2)$, the system (21) takes the form

$$\dot{\varepsilon}_1 = \varepsilon_2 \quad (22a)$$

$$\dot{\varepsilon}_2 = \zeta_1 + \zeta_2 \varepsilon_1 + \varepsilon_1^2 + s \varepsilon_1 \varepsilon_2 + O(\|\varepsilon\|^3) \quad (22b)$$

where $s = \text{sign}(l_{20}(k_{20}(0) + l_{11}(0)))$, $\zeta_1(\eta) = \frac{S^4(\eta)}{R^3(\eta)} \kappa_1(\eta)$, $\zeta_2(\eta) = \frac{S^2(\eta)}{R^2(\eta)} \kappa_2(\eta)$.

In order to define an invertible smooth change of parameters near $\eta = 0$, we also assume $\det(\frac{\partial \beta}{\partial \eta}(\eta = 0)) \neq 0$ (BT ... 3). Hence, the system (4) experiences the Bogdanov-Takens bifurcation when (η_1, η_2) is small in the neighbourhood of $(0, 0)$ (which is equivalent to (β, h) in the neighbourhood of $(\beta^{[BT]}, h^{[BT]})$). According to [43] the local representation of the three different bifurcation curve (SN, H, and HL) are given below for the small values of (η_1, η_2) .

Saddle-node Bifurcation curve:

$$\begin{aligned} SN &= \{(\eta_1, \eta_2) : 4\zeta_1(\eta_1, \eta_2) - (\zeta_2(\eta_1, \eta_2))^2 = 0\} \\ &= \{(\beta, h) : 4\zeta_1(\beta - \beta^{[BT]}, h - h^{[BT]}) - (\zeta_2(\beta - \beta^{[BT]}, h - h^{[BT]}))^2 = 0\} \end{aligned}$$

Hopf bifurcation curve:

$$\begin{aligned} H &= \{(\eta_1, \eta_2) : \zeta_1(\eta_1, \eta_2) = 0, \zeta_2 < 0\} \\ &= \{(\beta, h) : \zeta_1(\beta - \beta^{[BT]}, h - h^{[BT]}) = 0\} \end{aligned}$$

Homoclinic Bifurcation curve:

$$\begin{aligned} HL &= \{(\eta_1, \eta_2) : \zeta_1(\eta_1, \eta_2) = -\frac{6}{25}(\zeta_2(\eta_1, \eta_2))^2, \zeta_2 < 0\} \\ &= \{(\beta, h) : \zeta_1(\beta - \beta^{[BT]}, h - h^{[BT]}) = -\frac{6}{25}(\zeta_2(\beta - \beta^{[BT]}, h - h^{[BT]}))^2\} \end{aligned}$$

The curve SN divides the plane $\beta - h$ in two zones, one of them contains two interior equilibrium points and the other has no equilibria and on this curve there exists a unique coincident equilibrium point. The curve H corresponds to the existence of Hopf bifurcation and HL for the existence of a homoclinic Loop.

6 Numerical results and discussion

In this section, we shall justify all the theoretical findings of the model system (4) that we have obtained in the previous sections by numerical simulation. To perform the numerical simulations the parameters are chosen hypothetically (see Table 2) and we use the MAPLE and MATLAB software. We have already seen that the number and nature of equilibrium points are varying with the variation of parameters h , β and α . For different values of the parameters h , β and α , the trivial and axial equilibrium points always exist but the number of interior equilibrium point varies. There may be no interior equilibrium point, one coincident interior equilibrium point, two distinct interior equilibrium point and only one interior equilibrium point for different values of h , β and α .

Usually we investigate the dynamics of ecological models by considering the two-dimensional bifurcation diagram with two of the model parameters as the bifurcation parameters and fixing the others. Here, we are investigating the dynamics of the proposed model by considering a three-dimensional bifurcation diagram (see Figure 2(a), (b)) to study the dependency of the proposed model on the three significant model parameters h , β and α . Figure 2(a) represents the schematic bifurcation diagram in the first octant of the $h - \beta - \alpha$ co-ordinate system. To identify the surfaces clearly we filled the surfaces by the corresponding colors as shown in Figure 2(b) and a cross-section in two dimensions considering h and β as the bifurcation parameters is presented in Figure 2(c).

In Figure 2(a), (b) the red, blue, cyan, green surfaces and the black line correspond to the saddle-node, Hopf, homoclinic, transcritical bifurcation surfaces and Bogdanov-Takens bifurcation curve in $h - \beta - \alpha$ three-dimensional space, with other parameters being fixed as given in Table 2. It is clear from Figure 2(a), (b) that the first octant of $h - \beta - \alpha$ surface divides into six separate sub-spaces having no, one or two interior equilibrium points with different nature (nature of the axial equilibrium points also varies in the different spaces). We are now naming the different sub-spaces by S_1, S_2, S_3, S_4, S_5 and S_6 as shown in Figure 2(a), (b). In the sub-space S_1 , there do not exist any interior equilibrium point, only the trivial and the axial equilibrium points exist here. Along with the trivial and axial equilibrium points, two interior equilibrium points arise in S_2, S_3, S_4 . The interior equilibrium point with a lower density level of the predator species is always saddle and the other with a higher density level of predator species is a stable spiral, unstable spiral with a stable limit cycle around the equilibrium point and unstable spiral with no limit

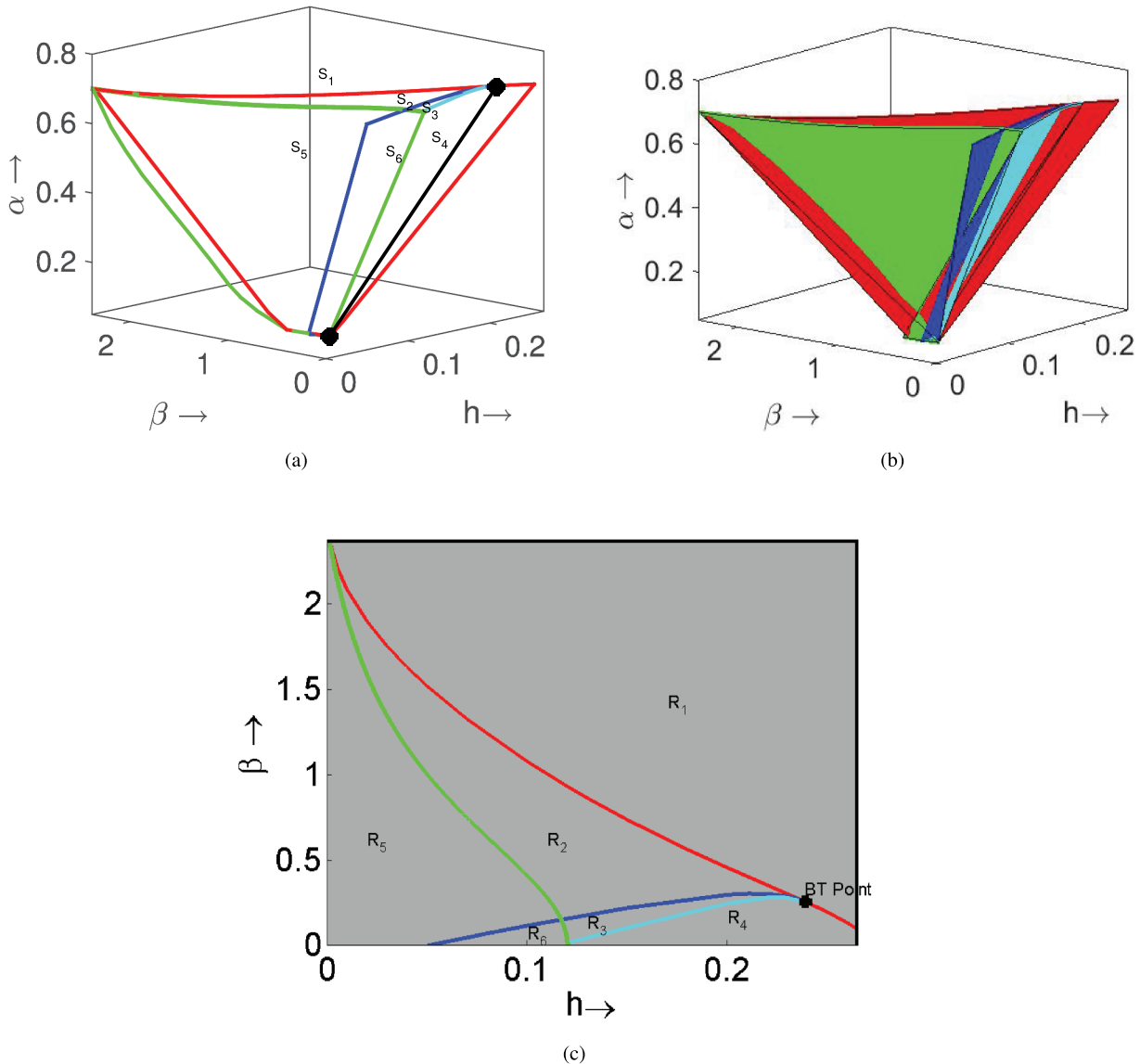


Figure 2. Figure 2: (a) The schematic bifurcation diagram of the system (4) in the first octant of the $h - \beta - \alpha$ co-ordinate system with parametric values as given in Table 2. The red, blue, cyan, green surfaces and the black line represent respectively the saddle-node bifurcation surface, Hopf bifurcation surface, homoclinic bifurcation surface for the interior equilibrium point, transcritical bifurcation surface for the axial equilibrium point and Bogdanov-Takens bifurcation line respectively, (b) the bifurcation surfaces in Figure 2(a) are filled by corresponding colors and (c) the cross-section of three-dimensional bifurcation diagram by the plane $\alpha = 0.7$.

cycle around the equilibrium point in the sub-spaces S_2 , S_3 and S_4 respectively. The sub-spaces S_5 , S_6 contain only one interior equilibrium point which is a stable spiral in S_5 and an unstable spiral with a stable limit cycle in S_6 .

It is clear from Figure 2, that there are no interior equilibrium points below the plane $\alpha = 0.112$ and with the increase of dimensionless conversion efficiency (α) the stability space of the interior equilibrium point increases. Biologically, if the conversion efficiency (α) increases then density of the predator populations

increase and consequently the system allows higher harvesting efficiency such that both the species survive with this higher amount of harvesting. It is also clear from the figures that for a higher value of (α) and moderate values of the environmental protection parameter of prey (β) and lower values of (h) the system shows less complex dynamics (as in the sub-space S_5) compare to dynamics with higher values of (h).

In Figure 2(c), we have presented the two-dimensional cross-section (in $h - \beta$ plane) of the three-dimensional bifurcation diagram corresponding to

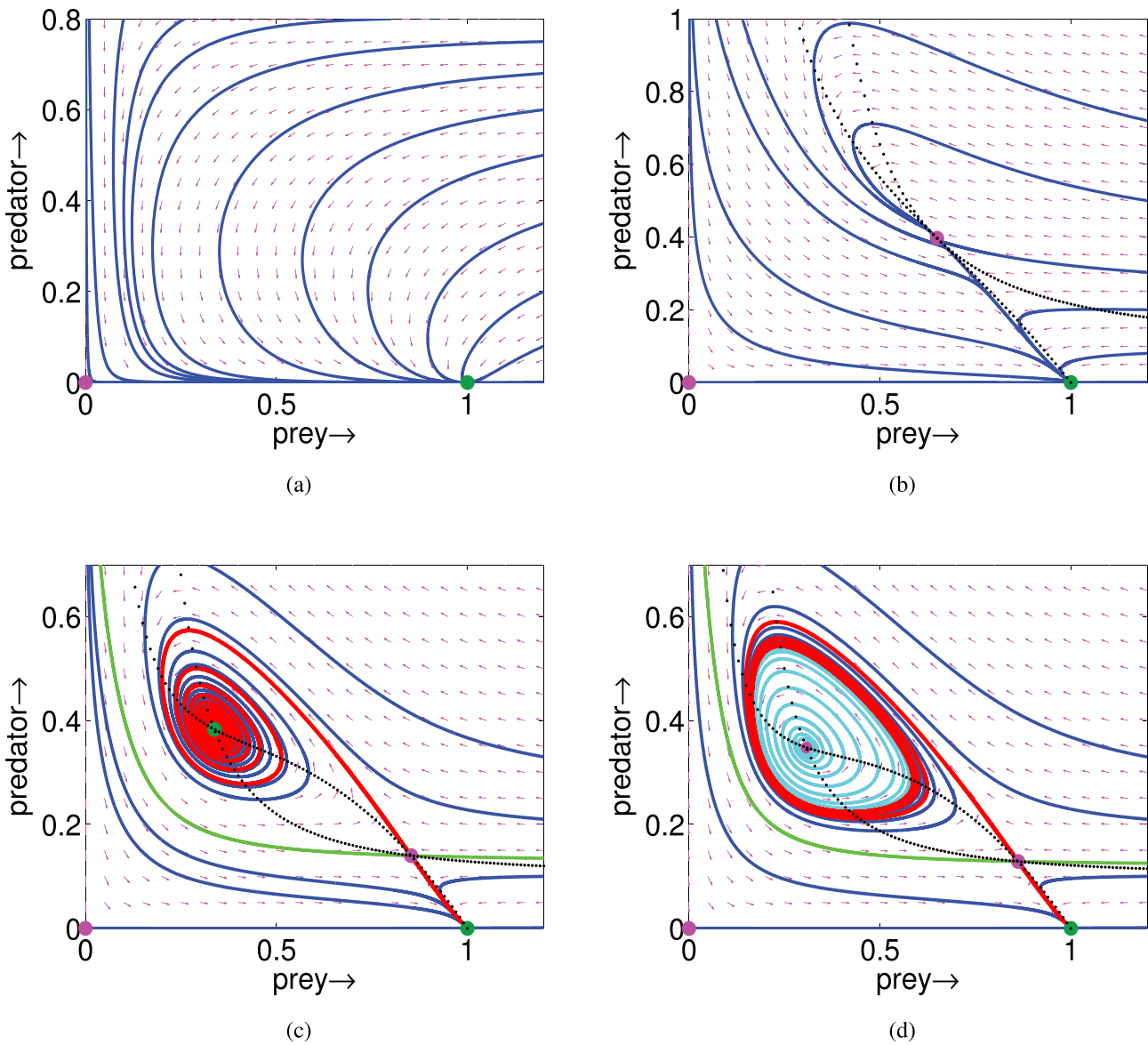


Figure 3. The phase diagram of the system (4) for the values of different parameters as given in Table 2 with (a) $h = 0.58$, $\beta = 0.18$, in sub-region R_1 ; (b) $h = 0.18$, $\beta = 0.5598348639$, on the saddle-node bifurcation curve; (c) $h = 0.18$, $\beta = 0.285$, in sub-region R_2 ; (d) $h = 0.18$, $\beta = 0.245$, in sub-region R_3 ; here black dotted lines denote the nullclines.

$\alpha = 0.7$. According to the existence of the equilibrium points and their nature, the first quadrant of $h - \beta$ plane divides into six sub-regions namely $R_i, (i = 1, 2, 3, 4, 5, 6)$ as shown in Figure 2(c) and these regions are the corresponding cross-sections of the sub-spaces $S_i, (i = 1, 2, 3, 4, 5, 6)$ for $\alpha = 0.7$. Here, to investigate the nature of the various equilibrium points for different values of the parameters in various sub-regions we have drawn the phase portrait of the system (4) in the next paragraphs.

Now, we start from the sub-region R_1 of Figure 2(c). In this sub-region, only trivial and axial equilibrium points exist. The trivial equilibrium point is a saddle and the axial equilibrium point is a stable node here (see

in Figure 3(a)). In this sub-region, only prey species can survive as there is no interior equilibrium point. From the biological point of view, this region is not so significant.

Then we enter in the sub-region R_2 from the sub-region R_1 , we have to cross the saddle-node bifurcation curve (red line in Figure 2(c)), on which the two interior equilibrium points coincide into a single interior equilibrium point. The corresponding phase diagram on this line is given by Figure 3(b). In the sub-region R_2 , along with the trivial and axial equilibrium points two distinct interior equilibrium points exist. Here, the nature of trivial and axial equilibrium point is the same as in R_1 and the interior equilibrium point with a lower density

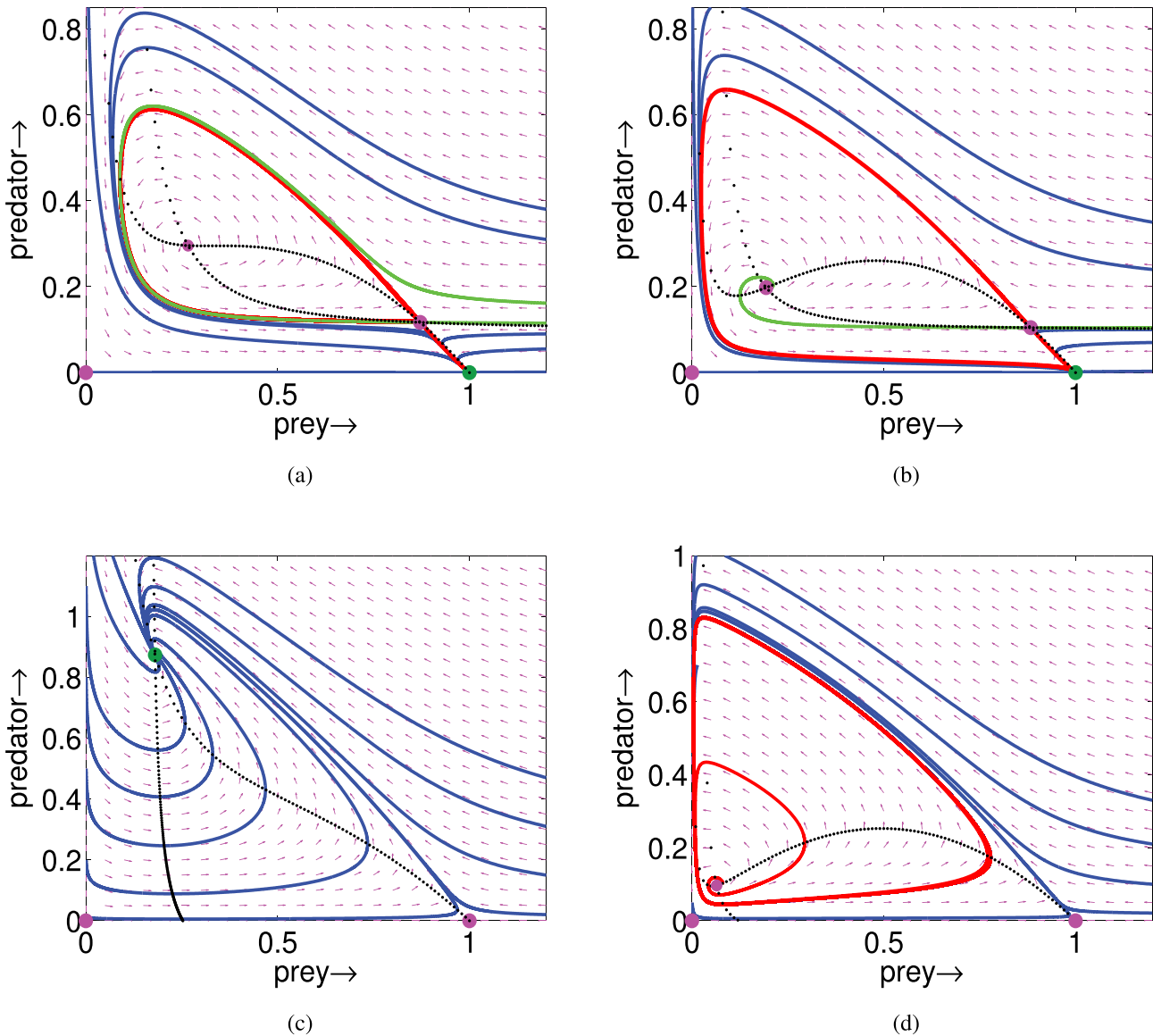


Figure 4. The phase diagram of the system (4) for the values of different parameter as given in Table 2 with (a) $h = 0.18$, $\beta = 0.190743$, on the homoclinic bifurcation curve; (b) $h = 0.18, \beta = 0.1$, in sub-region R_4 ; (c) $h = 0.02, \beta = 0.4$, in sub-region R_5 ; (d) $h = 0.1, \beta = 0.05$, in sub-region R_6 , here black dotted lines denote the nullclines.

level of the predator species is a saddle and the other with a higher density level of predator species is a stable spiral. The corresponding phase portrait of the system (4) in the sub-region is shown in Figure 3(c). The system shows bi-stability nature in this sub-region: the points are the stable axial and the stable interior equilibrium point. If we take the values of the parameters in this sub-region, then the solution curve of the system (4) either goes to the asymptotically stable interior equilibrium point or will attract by the stable axial equilibrium point. This sub-region is very significant from the biological point of view because if we take the initial amount of the prey and predator species above a threshold value, both the species can survive together

with a positive density level for a long time. Therefore the population biologist can suggest to take the values of the parameters in this sub-region for the co-exist of both species long time. Next, we enter into the sub-region R_3 by crossing the Hopf bifurcation line (blue line in Figure 2(c)).

In the sub-region R_3 , the number of the equilibrium point is the same as in the sub-region R_2 and the nature of the trivial and axial equilibrium point is also the same as in the previous sub-region. But the equilibrium point which was a stable spiral in the sub-region R_2 becomes an unstable spiral and finally attracting by a stable limit cycle around it (see Figure 3(d)). The nature of other interior equilibrium point in this sub-region shows the

same behaviour like as in the sub-region R_2 (saddle point). From the biological point of view, this sub-region is also important because both the species can survive simultaneously here. Depending on the initial population density, the solution either oscillates periodically around the interior equilibrium point or is attracting to the predator-free equilibrium point.

Then, to enter into the region R_4 from the region R_3 , we have to cross the homoclinic bifurcation line (cyan line). On the homoclinic bifurcation line, the limit cycle around the interior equilibrium point (unstable spiral in the previous region) becomes larger and connects the saddle interior equilibrium point, as a result one homoclinic loop arises. The phase portrait of the system (4) on this line is represented by Figure 4(a). In the sub-region R_4 , the number of the equilibrium point is the same like the previous sub-region (R_3) and also the nature of trivial and axial equilibrium point is the same as the previous. In this sub-region the homoclinic loop disappears and the system converges to the predator-free equilibrium point (see Figure 4(b)). This sub-region is biologically dangerous because both the species can not survive together, the predator population goes to extinction.

Next, we enter into the sub-region R_5 crossing the transcritical bifurcation line (green line) from the sub-region R_2 . In this sub-region the saddle interior equilibrium point disappears and the axial equilibrium point becomes unstable through the transcritical bifurcation. Here both axial and trivial equilibrium points are saddle and the interior equilibrium point is the stable focus (see Figure 4(c)). Finally, if we enter into the sub-region R_6 from the sub-region R_5 then the number of the equilibrium point is the same as the sub-region R_5 . Here the nature of the trivial and axial equilibrium point is also the same as the previous sub-region but the stable interior equilibrium point becomes an unstable spiral and a stable limit cycle arises around it (see Figure 4(d)). Thus, the two sub-regions (R_5, R_6) are most significant from a biological point of view because the survival of both the species is possible here without any restrictions. The solution curves starting anywhere in this sub-region are either attracting to the interior equilibrium point or oscillates with a positive density level.

7 Concluding remarks

In this present paper, we have considered a two-dimensional prey-predator model with Holling type III functional response and non-linear predator harvesting.

We have established that the system solution is positive and bounded. Along with the trivial and predator-free equilibrium points the system has at most two interior equilibrium points depending on values of the model parameters. The local asymptotic stability of different equilibrium points and the global stability of the interior equilibrium points are discussed here. The trivial equilibrium point is always unstable, which implies that the system can never be collapsed for any values of the system parameters. The predator-free equilibrium point is locally asymptotically stable under some parametric restrictions. There exists a set of values of the system parameters for which the interior equilibrium point is locally asymptotically stable, i.e. both the populations can survive with positive density level.

We have observed that the system goes through different bifurcation like saddle-node, transcritical, Hopf and Bogdanov-Takens bifurcation. In the biological point of view, these bifurcations are of great importance. Through saddle-node bifurcation, the system generates two interior equilibrium points among them one is always saddle and the other is stable or unstable spiral under depending on parameter values. Through transcritical bifurcation, the predator-free equilibrium point exchanges its stability with an interior equilibrium point. There is a critical value of the non-dimensional harvesting rate above which the extinction probability of the predator populations becomes prominent. The system shows complex dynamical behaviour in the neighbourhood of the Bogdanov-Takens bifurcation singularity in two-dimensional bifurcation plane.

Numerical simulations have been carried out to justify the mathematical findings. A three-dimensional bifurcation diagram has been constructed to observe the impact of three significant system parameters on the model system together. The three-dimensional surface is divided into seven disjoint sub-surfaces by different bifurcation surfaces, in which the number and nature of the equilibrium point are different. The nature of the solutions in two-dimensional bifurcation plane with a cross-section of this three-dimensional bifurcation diagram by $\alpha = 0.7$ plane is studied extensively. It is clear from the whole analysis that the harvesting has a great biological impact on the model system. From an economical point of view, this article has great significance. It will be more helpful to the experimental ecologist to understand the ecological phenomena and performing their works on more realistic problems. It will also be helpful to the business person to make a proper harvesting policy such that both the species co-

exist simultaneously.

Acknowledgements

The authors would like to thank the anonymous reviewers for their careful reading, useful comments and constructive suggestions for the improvement of the manuscript of the present research work.

Disclosure statement

No potential conflict of interest was reported by the author.

Notes on contributors

Prahlad Majumdar is a research scholar of Department of Applied Mathematics, University of Calcutta, Kolkata, India. He is working on the mathematical modelling on ecological systems with different biological effect. He has one publication in a reputed international journal.

Surajit Debnath is currently a research scholar of Department of Applied Mathematics, University of Calcutta, Kolkata, India. He is mainly interested in application of dynamical system in different topic of prey-predator model. He has one publication in a reputed international journal.

Susmita Sarkar is a Professor of Applied Mathematics at the University of Calcutta. Her field of research includes plasma dynamics, biomathematics, and fractional calculus. She has more than 100 research publications in reputed international journals. She is also associated with TWAS and ICTP.

Uttam Ghosh is an assistant professor of Applied Mathematics in University of Calcutta. His research includes Biomathematics and Fractional calculus. He has 64 publications in reputed national and international journals.

ORCID

Uttam Ghosh  <http://orcid.org/0000-0001-7274-7793>

References

- [1] Clark CW, DePree JD. A simple linear model for the optimal exploitation of renewable resources. . *Applied Mathematics and Optimization*. 1979;5(1):181–196.
- [2] Clark CW. Mathematical Models in the Economics of Renewable Resources. *SIAM Review*. 1979;21(1):81–99.
- [3] Mesterton-Gibson M. A technique for finding optimal two-species harvesting policies. . *Ecological Modelling*. 1996;92(2–3):235–244.
- [4] Clark CW. Mathematical Bieconomic: the Optimal Management of Renewable Resources. USA: Princeton University Press; 1976.
- [5] Clark CW. Bieconomic Modelling and Fisheries Management. New York: Wiley; 1985.
- [6] Panja P. Combine effects of square root functional response and prey refuge on predator-prey dynamics. International Journal of Modelling and Simulation. 2020;1–8. DOI. [10.1080/02286203.2020.1772615](https://doi.org/10.1080/02286203.2020.1772615)
- [7] Perumal R, Munigounder S, Mohd MH, et al. Stability analysis of the fractional-order prey-predator model with infection. International Journal of Modelling and Simulation. 2020;1–17 DOI. [10.1080/02286203.2020.1783131](https://doi.org/10.1080/02286203.2020.1783131)
- [8] Panja P. Dynamics of a fractional order predator-prey model with intraguild predation. International Journal of Modelling and Simulation. 2019;39(4):256–268.
- [9] Lotka AJ. Elements Physical Biology. Baltimore: Williams and Wilkins; 1925.
- [10] Volterra V. Variation and fluctuations of a number of individuals in animal species living together [Translation by Chapman R.N., 1931]. McGraw Hill: Animal Ecology; 1926. p. 409–448.
- [11] Rosenzweig ML, MacArthur RH. Graphical representation and stability conditions of predator-prey interactions. *Am Naturalist*. 1963;97(895):209–223.
- [12] Holling CS. The components of predation as revealed by a study of small-mammal predation of the European pine sawfly. *The Canadian Entomol*. 1959;91(5):293–320.
- [13] Holling CS. The functional response of predators to prey density and its role in mimicry and population regulation. *Memoirs of the Entomological Society of Canada. suppl.* 1965; S45. ;97(S45):5–60.
- [14] Holling CS. The functional response of invertebrate predators to prey density. *Memoirs of the Entomological Society of Canada*. 1966;98(S48):5–86.
- [15] Freedman HI. Deterministic Mathematical Models in Population Ecology. New York: Marcel Dekker; 1980.
- [16] Freedman HI, Wolkowicz GSK. Predator-prey systems with group defence: the paradox of enrichment revisited. *Bulletin of Mathematical Biology*. 1986;48(5–6):493–508.
- [17] Morozov AY. Emergence of Holling type III zoo plankton functional response: bringing together field evidence and mathematical modelling. *Journal of Theoretical Biology*. 2010;265:45–54.
- [18] Jiang Z, Zhang W, Zhang J, et al. Dynamical Analysis of a Phytoplankton-Zooplankton System with Harvesting Term and Holling III Functional Response. *Int J Bifurcation Chaos*. 2018;28(13):13–23.
- [19] Kempf A, Floeter J, Temming A. Predator-prey overlap induced Holling type III functional response in the North Sea fish assemblage. *Marine Ecology Progress Series*. 2008;367:295–308.
- [20] Dubey B, Patra A and Upadhyay R. K. Dynamics of Phytoplankton, Zooplankton and Fishery Resource Model. *Applications and Applied Mathematics: An International Journal*. 2014;9:217–245.
- [21] Das T, Mukherjee RN, Chaudhuri KS. Bioeconomic harvesting of a prey-predator fishery. . *Journal of Biological Dynamics*. 2009;3(5):447–462.
- [22] Xiao S, Ruan S. Bogdanov-Takens bifurcations in predator-prey systems with constant rate harvesting. *Fields Institute Communications*. 1999;21:493–506.
- [23] Zhang X, Chen L, Neumann AU. The stage-structured predator-prey model and optimal harvesting policy. *Math Biosci*. 2000;168(2):201–210.
- [24] Hsu SB, Hwang TW, Kuang Y. Global dynamics of a predator-prey model with Hassell-Varley type

- functional response. Discrete and Continuous Dynamical Systems Ser B. **2008**;10:857–871.
- [25] Krishna SV. Conservation of an ecosystem through optimal taxation. . Bulletin of Mathematical Biology. **1998**;60(3):569–584.
- [26] Pradhan T, Chaudhuri KS. Bioeconomic harvesting of a schooling fish species: A dynamic reaction model. Korean Journal of Computational & Applied Mathematics. **1999**;6(1):127–141.
- [27] Srinivasu PDN. Bioeconomics of a renewable resource in presence of a predator. Nonlinear Analysis: Real World Applications. **2001**;2(4):497–506.
- [28] Lin CM, Ho CP. Local and global stability for a predator-prey model of modified Leslie-Gower and Holling-type II time delay. Tunghai, Science. **2006**;8:33–61.
- [29] Li Y, Xiao D. Bifurcations of a predator-prey system of Holling and Leslie types. Chaos, Solitons & Fractals. **2007**;34(2):606–620.
- [30] Zhang N, Chen F, Su Q, et al. Dynamic behaviours of a harvesting Leslie-Gower predator-prey model. Discrete Dynamics in Nature and Society Article ID. **2011**;473949:14.
- [31] Dai G, Tang M. Coexistence Region and Global Dynamics of a Harvested Predator-Prey System. SIAM Journal on Applied Mathematics. **1998**;58(1):193–210.
- [32] Kar TK, Matsuda H. Global dynamics and controllability of a harvested prey-predator system with Holling type III functional response. Nonlinear Analysis: Hybrid Systems. **2007**;1(1):59–67.
- [33] Chaudhuri KS. Dynamic optimization of combined harvesting of a two-species fishery. Ecol Model. **1988**;41(1–2):17–25.
- [34] Xiao D, Jennings L. Bifurcations of a Ratio-Dependent Predator-Prey System with Constant Rate Harvesting. SIAM Journal on Applied Mathematics. **2005**;65(3):737–753.
- [35] Peng GJ, Jiang YL, Li CP. BIFURCATIONS OF A HOLLING-TYPE II PREDATOR-PREY SYSTEM WITH CONSTANT RATE HARVESTING. International Journal of Bifurcation and Chaos. **2009**;19(08):2499–2514.
- [36] Lenzini P, Rebaza J. Non-constant predator harvesting on a ratio dependent predator-prey model. Applied Mathematics Science. **2010**;4:791–803.
- [37] Gupta RP, Chandra P, Banerjee M. Dynamical complexity of a prey-predator model with nonlinear predator harvesting. Discrete & Continuous Dynamical Systems - B. **2015**;20(2):423–443.
- [38] Hu D, Cao H. Stability and bifurcation analysis in a predator-prey system with Michaelis-Menten type predator harvesting. Nonlinear Analysis: Real World Applications. **2017**;33:58–82.
- [39] Matsuda H, Katsukawa T. Fisheries management based on ecosystem dynamics and feedback control. Fisheries Oceanography. **2002**;11(6):366–370.
- [40] LaSalle J. The Stability of Dynamical Systems. SIAM. **1976**.
- [41] Perko L. Differential Equations and Dynamical Systems. New York: Springer; **1996**.
- [42] Debnath S, Ghosh U, Sarkar S. Global dynamics of a tritrophic food chain model subject to the Allee effects in the prey population with sexually reproductive generalized-type top predator. Computational and Mathematical Methods 2. **2019**; 2:e1079.
- [43] Kuznetsov YA. Applied Mathematical Sciences. Elements of Applied Bifurcation Theory. . Springer. New York. N. : ; **1995**. p. 112 .
- [44] Sen D, Ghorai S, Sharma S, et al. Allee effect in prey's growth reduces the dynamical complexity in prey-predator model with generalist predator. Appl Math Modell. **2021**;91:768–790.

Appendices

Appendix-I

From the first equation of (4), we have $\frac{dx}{dt} \leq x(1-x)$, from this inequality we have $\lim_{t \rightarrow \infty} \sup x(t) \leq 1$. Using this value in the second equation of (4) we have the following:

$$\begin{aligned} \frac{dy}{dt} &\leq y \left[\frac{\alpha}{\beta^2} - \delta - \frac{h}{g+y} \right] \leq y \left[\frac{\left(\frac{\alpha}{\beta^2} g - h \right) - \left(\delta - \frac{\alpha}{\beta^2} \right) y}{g+y} \right] \\ &\leq y \left[\frac{\left(\frac{\alpha}{\beta^2} g - h \right) - \left(\delta - \frac{\alpha}{\beta^2} \right) y}{g} \right] \end{aligned}$$

which gives $\lim_{t \rightarrow \infty} \sup y(t) \leq s$, where $s = \frac{\alpha g - \beta^2 h}{\beta^2 \delta - \alpha}$ with $\frac{\beta^2 h}{g} < \alpha < \beta^2 \delta$.

Again from the first equation of the system of equation (4), we have $\frac{dx}{dt} \geq x \left[1 - \frac{s}{\beta^2} - x \right]$. This inequality implies $\lim_{t \rightarrow \infty} \inf x(t) \geq v_1$, where $v_1 = 1 - \frac{s}{\beta^2}$ for $\beta^2 > s$.

Appendix-II

(a) Since interior equilibrium points are the intersection of the lines $y = f_1(x) = (1-x) \frac{\beta^2+x^2}{x}$ and $y = f_2(x) = \frac{h(\beta^2+x^2)}{(\alpha-\delta)x^2-\delta\beta^2} - g$ which are equivalent to $F_1 = 0$ and $F_2 = 0$. The interior equilibrium points coincides when the curves $y = f_1(x)$ and $y = f_2(x)$ touches each other, i.e. when $\frac{df_1(x)}{dx} \Big|_{E_2^*} = \frac{df_2(x)}{dx} \Big|_{E_2^*}$, where E_2^* is the coincident interior equilibrium point. Solving the above equation one can obtain the expression of $h^{[SN]}$ in terms of the steady state in the following form:

$$h^{[SN]} = \frac{((1-2x^*)x^{*2}-\beta^2)((\alpha-\delta)x^{*2}-\delta\beta^2)}{2x^{*3}\alpha}.$$

(b) Jacobian of the system (4) at the coincident interior equilibrium point E_2^* can be expressed as

$$J(E_2^*) = \begin{pmatrix} x \frac{\partial F_1}{\partial x} & x \frac{\partial F_1}{\partial y} \\ y \frac{\partial F_2}{\partial x} & y \frac{\partial F_2}{\partial y} \end{pmatrix}_{E_2^*}$$

If $\frac{dy^{(F_1)}}{dx}$ and $\frac{dy^{(F_2)}}{dx}$ denotes the slope of the tangents of the prey and predator nullclines at E_2^* then using implicit function theorem one can expressed [44]

$$\det(J(E_2^*)) = xy \frac{\partial F_1}{\partial y} \frac{\partial F_2}{\partial y} \left[\frac{dy^{(F_1)}}{dx} - \frac{dy^{(F_2)}}{dx} \right]_{E_2^*}.$$

Since at the saddle node bifurcation point i.e. at $h = h^{[SN]}$ both the nullclines touches each other and then $\frac{dy^{(F_1)}}{dx} = \frac{dy^{(F_2)}}{dx}$ which gives $\det(J(E_2^*)) = 0$.

Appendix-III

Expression of and d_{ij}

$$c_{11} = -\frac{(2x^* - \frac{2x^{*2}(\beta^2 x^* + x^{*3})}{(\beta^2 + x^{*2})^2})}{(\beta^2 + x^{*2})} c_{01} = -\frac{x^{*2}}{(\beta^2 + x^{*2})} c_{02} = 0$$

$$d_{21} = 0 d_{12} = -\frac{\frac{(a - \alpha x^*(\beta^2 x^* + x^{*3}))}{(\beta^2 + x^{*2})^2} - \frac{2\alpha\beta^2(2\beta^2 x^* + 2x^{*3})x^*}{(\beta^2 + x^{*2})^3}}{(\beta^2 + x^{*2})},$$

$$d_{03} = -\frac{h\gamma}{(\gamma + y^*)^4}$$

Appendix-IV

Expression of $a(\eta)$, $b(\eta)$, $c(\eta)$, $d(\eta)$, m_{ij} and n_{ij}

$$n_{00}(\eta) = -\delta y^* + \frac{\alpha x^{*2} y^*}{(\beta^{[BT]} + \eta_1)^2 + x^{*2}} - \frac{(h^{[BT]} + \eta_2)y^*}{(\gamma + y^*)} -$$

$$n_{02}(\eta) = \frac{(h^{[BT]} + \eta_2)\gamma}{(\gamma + y^*)^3}$$

$$n_{11}(\eta) = \frac{(2\alpha x^* - \frac{2\alpha x^{*2}((\beta^{[BT]})^2 x^* + 2\beta^{[BT]}\eta_1 x^* + \eta_1^2 x^* + x^{*3})}{((\beta^{[BT]})^2 + 2\beta^{[BT]}\eta_1 + \eta_1^2 + x^{*2})^2})}{((\beta^{[BT]} + \eta_1)^2 + x^{*2})}$$

$$n_{20}(\eta) = \frac{\alpha y^* - \frac{\alpha x^{*2} y^*}{((\beta^{[BT]})^2 + 2\beta^{[BT]}\eta_1 + \eta_1^2 + x^{*2})} - \frac{2\alpha x^{*2}(2(\beta^{[BT]})^2 y^* + 4\beta^{[BT]}\eta_1 y^* + 2\eta_1^2 y^*)}{((\beta^{[BT]})^2 + 2\beta^{[BT]}\eta_1 + \eta_1^2 + x^{*2})^2}}{((\beta^{[BT]} + \eta_1)^2 + x^{*2})}$$

Appendix-V

Expression of k_{ij} and l_{ij}

$$k_{00}(\eta) = \frac{m_{00}(\eta)}{p_{12}} - p_{11} \frac{m_{00}(\eta)}{p_{12}} - p_{00}(\eta)$$

$$k_{10}(\eta) = \frac{a(\eta)p_{12} - b(\eta)p_{11}}{p_{12}} - p_{11} \left\{ \frac{a(\eta)p_{12} - b(\eta)p_{11}}{p_{12}} + \frac{c(\eta)p_{12} - d(\eta)p_{11}}{p_{11}} \right\}$$

$$k_{01}(\eta) = \frac{a(\eta)p_{12} + b(\eta)(1 - p_{11})}{p_{12}} - p_{11} \left\{ \frac{a(\eta)p_{12} + b(\eta)(1 - p_{11})}{p_{12}} + \frac{c(\eta)p_{12} + d(\eta)(1 - p_{11})}{p_{11}} \right\} - 1$$

$$k_{20}(\eta) = 2 \frac{m_{20}(\eta)p_{12}^2 - m_{11}(\eta)p_{12}p_{11} + m_{02}(\eta)p_{11}^2}{p_{12}} - 2p_{11} \frac{m_{20}(\eta)p_{12}^2 - m_{11}(\eta)p_{12}p_{11} + m_{02}(\eta)p_{11}^2}{p_{12}} + 2n_{11}(\eta)p_{12}p_{11} - 2n_{02}(\eta)p_{11}^2$$

$$k_{02}(\eta) = 2 \frac{m_{20}(\eta)p_{12}^2 + m_{11}(\eta)p_{12}(1 - p_{11}) + m_{02}(\eta)(1 - p_{11})^2}{p_{12}} - 2p_{11} \frac{m_{20}(\eta)p_{12}^2 + m_{11}(\eta)(1 - p_{11}) + m_{02}(\eta)(1 - p_{11})^2}{p_{12}} - 2n_{11}(\eta)p_{12}(1 - p_{11}) - 2n_{02}(\eta)(1 - p_{11})^2$$

$$l_{00}(\eta) = \frac{p_{11}m_{00}(\eta)}{p_{12}} + n_{00}(\eta)$$

$$l_{10}(\eta) = p_{11} \left\{ \frac{a(\eta)p_{12} - b(\eta)p_{11}}{p_{12}} + \frac{c(\eta)p_{12} - d(\eta)p_{11}}{p_{11}} \right\}$$

$$l_{01}(\eta) = p_{11} \left\{ \frac{a(\eta)p_{12} + b(\eta)(1 - p_{11})}{p_{12}} + \frac{c(\eta)p_{12} + d(\eta)(1 - p_{11})}{p_{11}} \right\}$$

$$l_{20}(\eta) = 2p_{11} \frac{m_{20}(\eta)p_{12}^2 - m_{11}(\eta)p_{12}p_{11} + m_{02}(\eta)p_{11}^2}{p_{12}} - 2n_{11}(\eta)p_{12}p_{11} + 2n_{02}(\eta)p_{11}^2$$

$$l_{02}(\eta) = 2p_{11} \frac{m_{20}(\eta)p_{12}^2 + m_{11}(\eta)p_{12}(1 - p_{11}) + m_{02}(\eta)(1 - p_{11})^2}{p_{12}} + 2n_{11}(\eta)p_{12}(1 - p_{11}) + 2n_{02}(\eta)(1 - p_{11})^2$$